Focal deblending using smart subsets of OBN 5D data

Kontakis, A.; Verschuur, D. J.

Publication date
2017

Document Version
Final published version

Published in
79th EAGE Conference and Exhibition 2017

We P3 11

Focal Deblending Using Smart Subsets of OBN 5D Data

A. Kontakis* (Delft University of Technology), D.J. Verschuur (Delft University of Technology)

Summary

Although theoretically straightforward, adapting focal deblending to realistic 5D acquisition scenarios can be challenging in practice. The two main issues that have to be dealt with are insufficiently sampled spatial dimensions and the computational effort needed for the deblending inversion. In order to deal with both issues, we propose dividing the data in 'smart' subsets, specialized for the acquisition type. Then, the deblending problem can be divided into a number of smaller problems that can be solved independently. The focal transform used for the deblending is also redefined to fit the geometry of the subsets. We examine the case of OBN acquisition and test the performance of the proposed scheme on numerically blended field data.

Introduction

Simultaneous source acquisition, also referred to as blended acquisition, has matured enough as a technology to be used in the field. It offers extra flexibility to seismic acquisition by allowing a degree of overlap between the wavefields created by seismic sources. Therefore, it enables a tradeoff between shot density and acquisition time, which we can exploit in acquisition design. Other benefits include potential increase in the signal-to-noise ratio (SNR) of the recorded wavefields as well as incoherent illumination of the subsurface (Berkhout, 2008).

A considerable amount of effort has been devoted in answering key questions related to blended acquisition. The first important question is how to best manage the overlap between the recorded wavefields. The amount and nature of the overlap are controlled via the *blending code*, which specifies shot properties such as location, firing time, sweep parameters, amplitude modulation etc., always within the constraints posed by the type of aqcuisition and the seismic source technology to be used. A common choice is the random delay code, where random delays are introduced between each shot, the aim being to introduce incoherency in the blending noise. This technique can be extended by shot repetition, where each shot is repeated more than one time, which has the effect of amplifying the coherent signal compared to the incoherent blending noise (Wu et al., 2015). Source modulation can also give codes with properties favorable for separation (Robertsson et al., 2016).

The second important question is how to separate (deblend) the recorded wavefields. The main principle behind separation is to exploit properties of the blended signal that were specifically introduced by the blending code in order to aid the separation process. Usually the property exploited is the coherency of the signal versus the incoherency of the blending noise in the *pseudodeblended* wavefield, i.e. the wavefield after the adjoint of the blending operation has been applied. The separation process then can be posed as a problem of quantifying coherency somehow and accepting those solutions of the separation problem that maximize the chosen metric of coherency. The flexibility in defining a coherency metric has led to a variety of approaches to deblending. Examples include coherency-based FK filtering (Mahdad et al., 2011), median-based filtering (Gan et al., 2015; Zhan et al., 2015), sparsity-based methods using Radon transforms (Ibrahim and Sacchi, 2013; Haacke et al., 2015), curvelets (Lin and Herrmann, 2009; Wason et al., 2011) and seislets (Chen, 2015). Another approach is to use rank-reduction techniques (Wason et al., 2014; Cheng and Sacchi, 2015).

In Kontakis and Verschuur (2014) a deblending approach based on the double focal transform was introduced, with an application to a 2D line dataset. As discussed in Kontakis et al. (2016) and Kontakis and Verschuur (2016), extending this methodology for full 5D datasets presents a number of challenges, the most important being the computational cost involved in solving the inverse problem. Fortunately, it is possible to redefine the focal transform and tailor it for deblending 'smart' subsets of the 5D data volume. An application to the towed multi-streamer case was presented. In this paper we handle the case of an ocean bottom node (OBN) acquisition, as a continuation of the work found in Kontakis and Verschuur (2016), and demonstrate this on numerically blended field data.

Method and Theory

In an OBN acquisition typically a few receiver nodes are placed at the ocean bottom, while one or more vessels carrying seismic sources fire shots at the sea surface. Typically the number of shot locations is much greater than the number of receiver locations and usually follows a regular and dense grid. Applying the double focal transform (Berkhout and Verschuur, 2010; Kutscha et al., 2010; Kutscha and Verschuur, 2012) directly on the whole 5D data volume, apart from being computationally costly, would be very likely to introduce lots of artifacts due to the small number of receivers and the relatively big distance between them. Let $P(x_r, y_r, z_r; x_s, y_s, z_s; \omega) \equiv P(\mathbf{x}_r, \mathbf{x}_s; \omega)$ be a sample of the wavefield at angular frequency ω, generated by a source at $(x_s, y_s, z_s) \equiv \mathbf{x}_s$ and recorded by a receiver node at $(x_r, y_r, z_r) \equiv \mathbf{x}_r$. Note that since the acquisition under discussion is an OBN-type acquisition, z_r will generally be at the sea bottom, whereas $z_s = z_0 = 0m$ will be at the sea surface level.

A natural way to divide the recorded dataset into subsets, is to split the traces to sets, each one containing all traces with the same receiver coordinates. Thus, each subset pertains to a specific node and the deblending process to follow is understood to be performed separately for each of the subsets. Each of these subsets can be divided further into sets of traces $\mathscr{D}_m$, $m = 1, 2, \ldots, M$. The next step is to define

a focal transform for each set $\mathscr{D}_m$. Since we consider only one receiver and many sources, it is natural to do the focusing in the source dimension. The source-side single focal transform is suitable for this purpose. We assume a crude velocity model as prior knowledge. We can then define K depth levels z_k. For each of these depth levels and each set $\mathscr{D}_m$, a focal subdomain $X_{k,m}(\mathbf{x}_r;\mathbf{x}_f;\omega)$ - focal operator $G_{k,m}(\mathbf{x}_f;\mathbf{x}_s;\omega)$ pair can be defined such that

$$P_m(\mathbf{x}_r;\mathbf{x}_s;\omega) = \sum_{k=1}^{K} \sum_{\substack{\mathbf{x}_f \in \\ \mathscr{F}_{k,m}}} X_{k,m}(\mathbf{x}_r;\mathbf{x}_f;\omega) G_{k,m}(\mathbf{x}_f;\mathbf{x}_s;\omega), \qquad \mathbf{x}_r, \mathbf{x}_s \in \mathscr{D}_m. \tag{1}$$

The focal operator is a two-way wavefield extrapolator that extrapolates a wavefield from the source locations at the surface, to depth level z_k and then to a set of chosen coordinates $\mathscr{F}_{k,m}$ with elements $(x,y,z_r) \equiv \mathbf{x}_f$, that lie on the plane $z = z_r$, as schematically illustrated in Fig. 1a. The set of coordinates $\mathscr{F}_{k,m}$ defines a focusing grid. Generally we assume a homogeneous isotropic medium of known velocity for this extrapolation. The focal subdomain here can be understood as a virtual dataset with sources at $\mathbf{x}_f \in \mathscr{F}_{k,m}$ and a receiver at $\mathbf{x}_r \in \mathscr{D}_m$. This virtual dataset is produced by removing traveltime from the sources of $P_m(\mathbf{x}_r;\mathbf{x}_s;\omega)$. This has a focusing effect which can be later used to constrain the deblended solution. The focusing grid locations should be generally chosen to lie near the receiver coordinates for achieving good focusing. This could be the same for all depth levels, but it does not need to. In fact, for low focal velocities it can be beneficial to define a finer grid to avoid artifacts arising from the summation along $\mathbf{x}_f$ in Eq. (1). Similar to the towed streamer case, we pay a certain price for the simplifications we introduced. Approximate velocities, limited number of depth levels, a focusing grid of limited dimensions and working on a subset of the data, will generally lead to less good focusing than what could be achieved with a dense coverage of sources and receivers. Still, as will be seen in the example it is possible to achieve rather good separation despite these limitations.

For the blending part, we assume a random time delay code, where a source at location $\mathbf{x}_s$ fires at time $\tau(\mathbf{x}_s)$. The relationship between the blended and unblended data then is given by

$$P_{\mathrm{bl}}(\mathbf{x}_r;\mathscr{B}_i;\omega) = \sum_{\substack{\mathbf{x}_s \in \\ \mathscr{B}_i}} P_m(\mathbf{x}_r;\mathbf{x}_s;\omega) e^{-j\omega\tau(\mathbf{x}_s)}, \qquad m : (\mathbf{x}_s \in \mathscr{D}_m) \wedge (\mathbf{x}_s \in \mathscr{B}_i), \quad \mathbf{x}_r \in \mathscr{D}_m, \tag{2}$$

where $\mathscr{B}_i$ is the set of shots that generate the i-th blended shot gather. Inserting Eq. (1) in Eq. (2) we arrive at

$$P_{\mathrm{bl}}(\mathbf{x}_r;\mathscr{B}_i;\omega) = \sum_{\substack{\mathbf{x}_s \in \\ \mathscr{B}_i}} \sum_{k=1}^{K} \sum_{\substack{\mathbf{x}_f \in \\ \mathscr{F}_{k,m}}} X_{k,m}(\mathbf{x}_r;\mathbf{x}_f;\omega) G_{k,m}(\mathbf{x}_f;\mathbf{x}_s;\omega) e^{-j\omega\tau(\mathbf{x}_s)}, \; m : (\mathbf{x}_s \in \mathscr{D}_m) \wedge (\mathbf{x}_s \in \mathscr{B}_i), \; \mathbf{x}_r \in \mathscr{D}_m. \tag{3}$$

Using the matrix notation adopted in Berkhout (1982), Eq. (3) can be written more concisely using monochromatic frequency slices, where blended shots are stored as the columns of $\bar{\mathbf{P}}_{\mathrm{bl}}(z_r;z_s;\omega)$:

$$\bar{\mathbf{P}}_{\mathrm{bl}}(z_r;z_s;\omega) = \sum_{k=1}^{K} \bar{\mathbf{X}}_k(z_r;z_r;\omega) \bar{\mathbf{G}}_k(z_r;z_s;\omega) \bar{\mathbf{\Gamma}}(z_s;\omega). \tag{4}$$

The bar over the matrices serves as a reminder that we are working with a subset, rather than with the whole volume of the recorded dataset. The operator $\bar{\mathbf{\Gamma}}(z_s;\omega)$ performs the blending operation.

We can take advantage of the compression achieved by the focusing, by promoting sparse solutions in the compressed focal domain. A way to achieve this is to solve the following optimization problem:

$$\min \left\{ \sum_{t} \sum_{k=1}^{K} ||\bar{\mathbf{X}}_k(z_r;z_r;t)||_{\mathrm{S}} \right\} \text{ s.t. } \sum_{\omega} ||\bar{\mathbf{P}}_{\mathrm{bl}}(z_r;z_s;\omega) - \sum_{k=1}^{K} \bar{\mathbf{X}}_k(z_r;z_r;\omega) \bar{\mathbf{G}}_k(z_r;z_s;\omega) \bar{\mathbf{\Gamma}}(z_s;\omega)||_{\mathrm{F}} < \sigma. \tag{5}$$

Here $||\mathbf{A}||_S$ and $||\mathbf{A}||_F^2$ for a matrix $\mathbf{A}$ with elements A_{ij} are the sum norm and Frobenius norm respectively, with $||\mathbf{A}||_S = \sum_{i,j} |A_{ij}|$ and $||\mathbf{A}||_F = \sqrt{\sum_{i,j} |A_{ij}|^2}$. Note that in (5) the argument of the sum norm is in the time domain, since it is there where the solution is expected to be sparse. Solving (5) is a basis pursuit denoise (BPDN) problem, that can be efficiently solved by solvers such as SPGL1 (van den Berg and Friedlander, 2007, 2008).

Example

The deblending scheme is tested using a numerically blended dataset. The OBN acquisition scheme is depicted in Fig. 1b. Two source lines of 700 traces each from a particular receiver node were extracted and blended to form the blended dataset. The chosen receiver node and shot locations can be seen in red color in Fig. 1b. A total amount of approximately 3s was kept from the gathers, which contains frequencies up to 100Hz. The blending code used is a random time delay code of delays ranging from 0.1s to 0.4s. Six focal operators were used for deblending, with NMO velocities ranging from 1482m/s to 1800m/s and apex times from 0.7 to 2.08s. The unblended data (Fig. 1c) was made to be in the range of the operators before blending it. The pseudodeblended data can be seen in Fig. 1d and the deblended data in Fig. 1e. Most of the blending noise has been suppressed from the deblended result, something that can be also seen in the error section in Fig. 1f. The deblending quality is $Q = 19.8$dB, using the metric $Q = 10\log_{10}(\sum_t ||\bar{\mathbf{P}}_{\text{ideal}}(z_r;z_s;t)||_{\text{F}}^2 / \sum_t ||\bar{\mathbf{P}}_{\text{ideal}}(z_r;z_s;t) - \bar{\mathbf{P}}_{\text{debl}}(z_r;z_s;t)||_{\text{F}}^2)$.

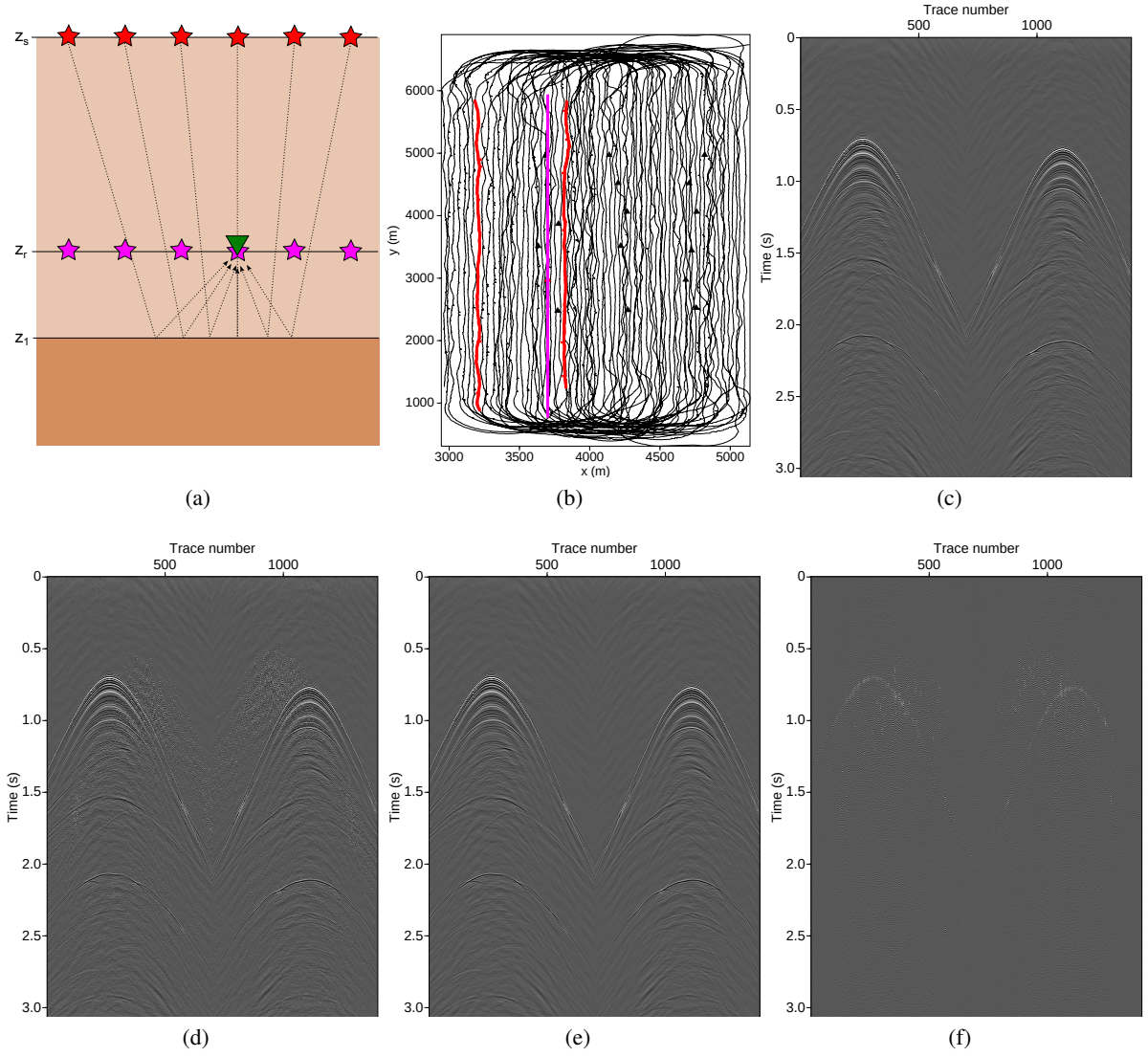

Figure 1: (a) Schematic representation of single-sided focusing, *red* original sources, *magenta* virtual sources at the focusing grid. The dotted traveltime is removed by the focal operator; (b) Acquisition plan for the field data, *red*: chosen node and sources, *magenta*: focusing grid; (c) Unblended data; (d) Pseudodeblended data; (e) Deblended data; (f) Deblending error, multiplied by 5.

Conclusions

Realistic acquisition will generally be subsampled in one or more dimensions, while still providing an amount of data that can make inversion-based seismic processing challenging. A way to reduce the

computational effort required for focal deblending is to use 'smart' subsets of data, breaking down a big inversion problem into several smaller ones that can be solved in parallel. An application of this idea to the case of OBN acquisition was presented, with encouraging results, paving the way for the application of focal deblending on realistic datasets.

Acknowledgments

The authors would like to thank sponsors of the Delphi consortium for their support, TEEC and GEOMAR for providing the field data and the authors of the SPGL1 solver for making it publicly available.

References

van den Berg, E. and Friedlander, M.P. [2007] SPGL1: A solver for large-scale sparse reconstruction. Http://www.cs.ubc.ca/labs/scl/spgl1.

van den Berg, E. and Friedlander, M.P. [2008] Probing the Pareto frontier for basis pursuit solutions. *SIAM Journal on Scientific Computing*, **31**(2), 890–912.

Berkhout, A.J. [1982] *Seismic migration, imaging of acoustic energy by wave field extrapolation, A: Theoretical aspects*. Elsevier (second edition).

Berkhout, A.J. [2008] Changing the mindset in seismic data acquisition. *The Leading Edge*, **27**(7), 924–938.

Berkhout, A.J. and Verschuur, D.J. [2010] Parameterization of seismic data using gridpoint responses. *80th SEG Annual International Meeting*, Expanded Abstracts, 3344–3348.

Chen, Y. [2015] Deblending by iterative orthogonalization and seislet thresholding. *85th SEG Annual International Meeting*, Expanded Abstracts, 53–58.

Cheng, J. and Sacchi, M.D. [2015] A fast rank-reduction algorithm for 3D deblending via randomized QR decomposition. *85th SEG Annual International Meeting*, Expanded Abstracts, 3830–3835.

Gan, S., Wang, S., Chen, X. and Chen, Y. [2015] Deblending using a structural-oriented median filter. *85th SEG Annual International Meeting*, Expanded Abstracts, 59–64.

Haacke, R., Hampson, G. and Golebiowski, B. [2015] Simultaneous shooting for sparse OBN 4D surveys and deblending using modified Radon operators. *77st EAGE Conference & Exhibition*, Extended Abstracts, We N101 08.

Ibrahim, A. and Sacchi, M.D. [2013] Simultaneous source separation using a robust Radon transform. *Geophysics*, **79**(1), V1–V11.

Kontakis, A. and Verschuur, D.J. [2014] Deblending via sparsity-constrained inversion in the focal domain. *76th EAGE Conference & Exhibition*, Extended Abstracts, Th ELI2 02.

Kontakis, A. and Verschuur, D.J. [2016] Focal deblending using smart subsets of towed streamer 5D data. *86th SEG Annual International Meeting*, Expanded Abstracts, 4612–4617.

Kontakis, A., Verschuur, D.J. and Wu, S. [2016] Acquisition geometry-aware focal deblending. *78th EAGE Conference & Exhibition*, Extended Abstracts, Th P4 05.

Kutscha, H. and Verschuur, D.J. [2012] Data reconstruction via sparse double focal transformation: An overview. *Signal Processing Magazine, IEEE*, **29**(4), 53–60.

Kutscha, H., Verschuur, D.J. and Berkhout, A.J. [2010] High resolution double focal transformation and its application to data reconstruction. *80th SEG Annual International Meeting*, Expanded Abstracts, 3589–3593.

Lin, T.T.Y. and Herrmann, F.J. [2009] Designing simultaneous acquisitions with compressive sensing. *71st EAGE Conference & Exhibition*, Extended Abstracts, S006.

Mahdad, A., Doulgeris, P. and Blacquière, G. [2011] Separation of blended data by iterative estimation and subtraction of blending interference noise. *Geophysics*, **76**(3), Q9–Q17.

Robertsson, J.O.A., Amundsen, L., Pedersen, Å.S., Eggenberger, K., Andersson, F. and van Manen, D.J. [2016] Wavefield signal apparition: Simultaneous source separation. *86th SEG Annual International Meeting*, Expanded Abstracts, 102–106.

Wason, H., Herrmann, F.J. and Lin, T.T.Y. [2011] Sparsity-promoting recovery from simultaneous data: a compressive sensing approach. *81st SEG Annual International Meeting*, Expanded Abstracts, 6–10.

Wason, H., Kumar, R., Herrmann, F.J. and Aravkin, A.Y. [2014] Source separation via SVD-free rank minimization in the hierarchical semi-separable representation. *84th SEG Annual International Meeting*, Expanded Abstracts, 120–126.

Wu, S., Blacquière, G., and van Groenestijn, G.J. [2015] Shot repetition: an alternative approach to blending in marine seismic. *85th SEG Annual International Meeting*, Expanded Abstracts, 120–126.

Zhan, C., Malik, R., Specht, J., Liu, Z. and Teixeira, D. [2015] Deblending of continuously recorded OBN data by subtraction integrated with a median filter. *85th SEG Annual International Meeting*, Expanded Abstracts, 4673–4677.